GEOPHYSICAL RESEARCH LETTERS, VOL. 35, L22309, doi:10.1029/2008GL035806, 2008

Importance of ocean tidal load corrections for differential InSAR

Christopher J. DiCaprio[1] and Mark Simons[1]

Received 25 August 2008; revised 15 October 2008; accepted 17 October 2008; published 29 November 2008.

[1] Large time series of interferometric synthetic aperture radar (InSAR) measurements make it possible to detect slow tectonic motions of the Earth's surface on the order of millimeters per year. Here, we illustrate the importance of correcting InSAR data for the effects of ground displacements due to ocean tidal loads (OTL). These loads can cause displacement gradients greater than 3 cm per 100 km, which is larger than the accuracy of InSAR techniques and can be a significant percentage of the measured displacement due to slow tectonic processes. We demonstrate the importance of OTL with predicted displacements from selected regions of tectonic interest. **Citation:** DiCaprio, C. J., and M. Simons (2008), Importance of ocean tidal load corrections for differential InSAR, *Geophys. Res. Lett.*, *35*, L22309, doi:10.1029/2008GL035806.

1. Introduction

[2] As the amount of available radar satellite data increases, we can better use interferometric synthetic aperture radar (InSAR) to study small amplitude deformation (on the order of millimeters per year) and to create long time series of surface motion [e.g., *Simons and Rosen*, 2007]. When using InSAR to measure small displacements, unwanted sources of deformation can be significant. Here, we focus on displacements from mass loading due to ocean tides, generally referred to as ocean tidal loading (OTL). OTL deformation is of particular concern when using InSAR to study processes occurring over length scales of order 100 km. Many sources of long-term deformation that we may be interested in studying can have wavelengths this scale or larger, including inter-seismic loading of seismogenic faults and post-seismic inelastic deformation.

[3] Other non-tectonic effects that we do not address in this paper include solid body tides, pole-tides, non-tidal mass loading both seasonal and non-seasonal, and ionospheric and tropospheric phase delay [e.g., *Simons and Rosen*, 2007]. The wavelength of solid body tides and pole tides are expected to be one to two orders of magnitude greater than the OTL [e.g., *Blewitt*, 2007]. They are therefore negligible in InSAR processing because at the scale of an interferogram they primarily introduce an additive constant to the phase; such constituents are not normally resolved in standard differential InSAR as interferometry only has the ability to measure relative displacement within an image. Generally, non-tidal, non-seasonal, mass loading is expected to be much smaller than the OTL signal near the coast and can be safely ignored in most InSAR analyses [*Dong et al.*, 2002]. Seasonal signals that are non-tidal may be significant for particular regions (e.g. those close to aquifers or glaciers), but they are not easily estimated generically and must be dealt with on a case-by-case basis.

[4] OTL displacements are the elastic response of the Earth to the redistribution of water mass from the ocean tides [e.g., *Agnew*, 2007]. OTL can introduce deformation gradients of several millimeters to centimeters across an interferogram near coastal regions, and therefore needs to be considered carefully. For example, in South-West England, vertical ground displacements due to tidal loading can range over 10 cm [*Penna et al.*, 2008] and displacement gradients can be larger than 3 cm per 100 km. Corrections for OTL displacements are commonly performed during analysis of GPS and VLBI time series [e.g., *Urschl et al.*, 2005], but are not currently considered for InSAR processing. The effect of the OTL is readily calculated using existing tools; thus, model predicted OTL should be subtracted from an interferogram before tectonic analysis. The dominant component of OTL displacement is vertical and the line of sight look angle of most SAR satellites makes them sensitive to vertical ground deformation (e.g. a representative look angle for ERS and Envisat is about 23 degrees from vertical).

[5] Even if we are not interested in long-wavelength deformation, the OTL signal may be of concern, since during InSAR processing it is common to re-estimate the satellite baseline. By re-estimating the baseline we aim to eliminate errors due to uncertainties in the satellite orbits. The re-estimation process removes long-wavelength signals from the interferogram, meaning that any real long-wavelength deformation, as well as any long-wavelength variation in propagation delay, would be mapped into the satellite baseline. If not removed, long-wavelength OTL deformation can cause errors in the baseline re-estimation process.

[6] Accounting for the OTL displacements in InSAR data analysis becomes more important as more radar satellite data becomes available, and we are able to measure slow processes. For example, a formal time series analysis of InSAR data would include, in addition to estimates of error, all known sources of deformation. Accounting for non-tectonic sources of deformation such as OTL can also help with more rigorous integration of InSAR with GPS observations.

2. Examples

[7] In order to calculate the displacement due to the ocean tidal loads we use the SPOTL software [*Agnew*, 1997]. Alternate means of computing the OTL include the "Ocean Tide Loading Provider" web site (http://www.oso.chalmers.se/loading/), which uses OLFG/OLMPP [*Scherneck*, 1991]; GOTIC2 [*Matsumoto et al.*, 2005]; and CARGA [*Bos and Baker*, 2005].

[1]Seismological Laboratory, California Institute of Technology, Pasadena, California, USA.

0094-8276/08/2008GL035806$05.00

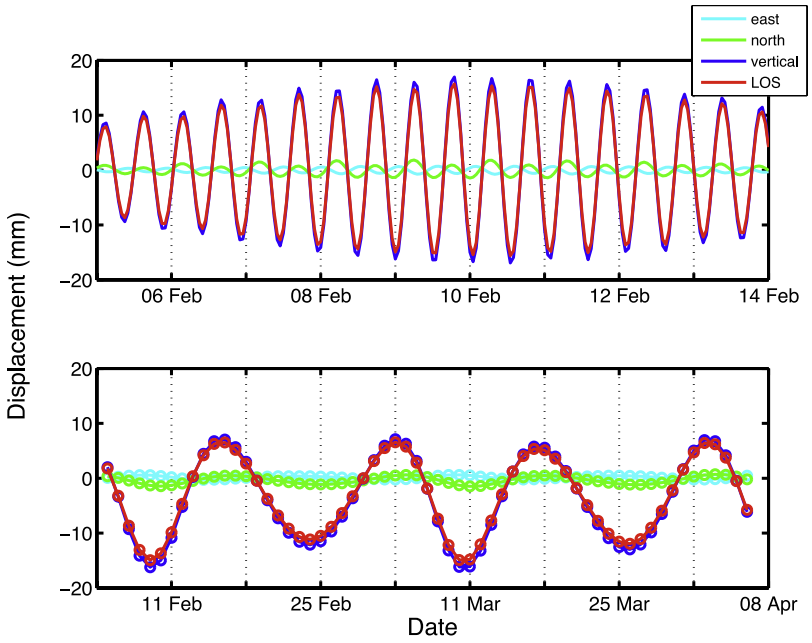

Figure 1. (top) Time series of relative displacements in northern Iceland due to OTL for a period in 2001. The displacements are taken at the point (16.30W, 66.27N) relative to (17.15W, 64.45N) giving the relative displacement north to south for a typical interferogram (see Figure 2). LOS (line of sight) is taken from the radar geometry of ERS track 1. (bottom) Time series sampled at the same time every day to demonstrate the shift in tidal maximum relative to the time of day. Note the different time scales and tick intervals for the two plots. Tick marks are at zero hours UTC.

[8] The SPOTL program nloadf calculates the OTL amplitude and phase for a specific tidal constituent at a particular location using any number of global and/or local tidal models and convolving the resultant water height with the Green's functions for the Earth's elastic response to mass loading. The program hartid uses the derived harmonic tide constituents and predicts the OTL displacement at a particular time. Several studies have compared OTL models to GPS data [*Thomas et al.*, 2007; *Melachroinos et al.*, 2007; *Vergnolle et al.*, 2008; *Penna et al.*, 2008]. *Penna et al.* [2008] showed that for particular GPS sites, removing the M2 OTL displacements predicted by the CARGA software can reduce the amplitude of displacements at the period associated with the M2 tide to the level of the noise in the GPS time series; although the ability of OTL models to correct geodetic data depends on many factors including location and required precision for the geological application. The SPOTL package has also been shown to accurately predict the OTL displacement. *Penna et al.* [2008] compared several OTL softwares and found that those that did not use water mass redistribution (including SPOTL) show no greater than 1–2 mm difference in predicted vertical displacements near the coast and discrepancies less than 0.2–0.5 mm inland.

[9] In all of the following examples, the amplitude and phase from tidal constituents M2, S2, N2, K2, K1, O1, P1, and Q1 for version 00.2 of the Goddard Ocean Tide Model (GOT00.2) [*Ray*, 1999] were input into hartid to calculate the displacement at a given time and location. GOT00.2 was chosen among several available modern ocean tide models. *Penna et al.* [2007] show that GOT00.2 and four other ocean tide models are in close agreement for the purpose of calculating OTL displacements in all regions considered in this paper. We used the elastic Green's functions from the Gutenberg-Bullen Earth Model [*Farrell*, 1972]. The examples shown are for regions of tectonic interest that have sizable OTL displacements.

[10] One should consider which tidal model is best for the region of interest [e.g., *Baker and Bos*, 2003; *Melachroinos et al.*, 2007; *Penna et al.*, 2007]. Commonly used modern ocean tidal models include CSR4.0 [*Eanes and Bettadpur*, 1995], FES2004 [*Lefevre et al.*, 2002], GOT00.2 [*Ray*, 1999], NAO99b [*Matsumoto et al.*, 2000], and TPXO6.2 [*Egbert and Erofeeva*, 2002]. *Thomas et al.* [2007] found that these models are indistinguishable within measurement noise for a small number of GPS stations. However, *Baker and Bos* [2003] state that no single ocean tide model is applicable to all parts of the world. *Penna et al.* [2007] map the scatter in OTL displacement predictions from several different tidal models and found that model discrepancies are particularly large near shallow seas. In addition, *Penna et al.* [2008] found that at several coastal sites the calculated OTL displacement is sensitive to the specific tide model used at the several millimeter level.

[11] In most differential InSAR applications we are only concerned with the relative displacements within a particular interferogram and not the absolute displacements. Figure 1 shows the relative displacements due to the OTL between two extremal points in a typical radar footprint as a function of time for northern Iceland. A given satellite typically images the same location at approximately the same time of day; such a sampling is shown in the bottom plot of Figure 1. Because the period of the tidal maximum is not twenty four hours, a different amplitude of the OTL

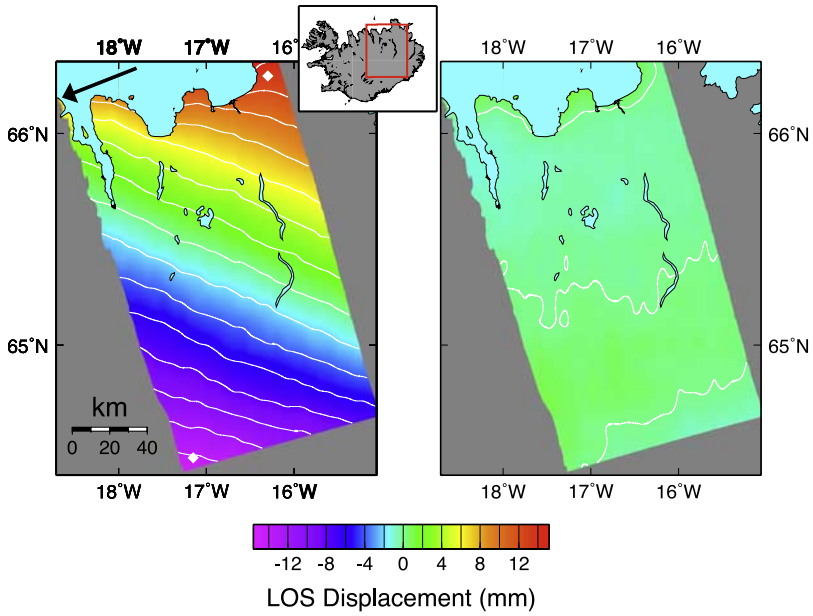

Figure 2. Synthetic interferogram of peak expected relative displacements due only to ocean tidal load displacements in northern Iceland. The displacement would be expected for a fictitious interferogram constructed from radar acquisitions at 2003-01-26 12:00:00 and 2002-03-29 12:00:00. The radar geometry is from track 1 of the ERS and Envisat satellites. The arrow indicates the surface projection of the approximate radar line of sight (LOS) direction from ground to satellite. LOS displacement is the projection of the displacement vector along the LOS direction. The two white diamonds indicate the points used to calculate relative displacements in Figure 1. (right) Residual after removing best fitting bi-linear ramp from predicted OTL displacement. Contour intervals are 2 mm.

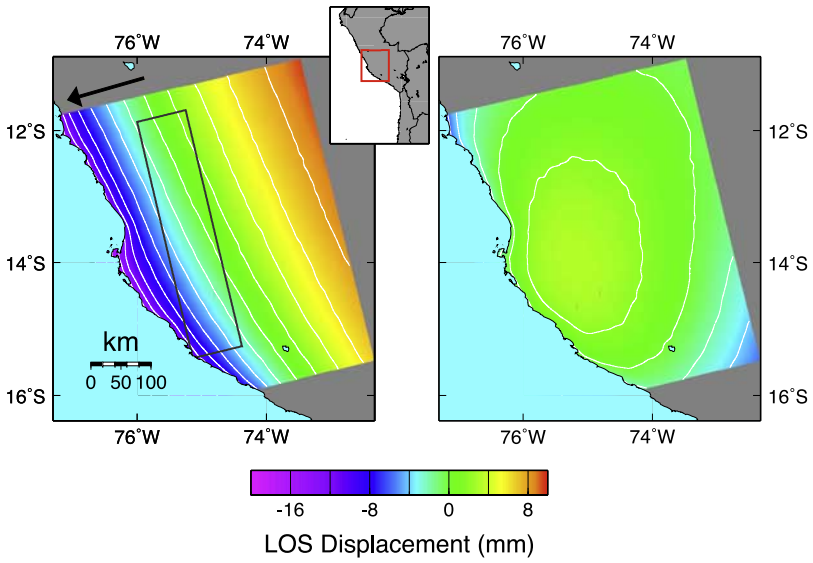

Figure 3. Same as Figure 2 for a wide swath scene of the Peruvian subduction zone. The gray box is the footprint of a normal strip-map swath. Acquisition times are 2004-07-03 12:00:00 and 2002-01-07 12:00:00. The radar geometry is from the wide swath track 447 of the Envisat satellite. Contour intervals are 2 mm.

displacement is sampled each day. A particular SAR pair is usually chosen based on the geophysical target and available data without regard to the magnitude of the OTL displacement across the interferogram; therefore, InSAR users are likely to encounter the maximum OTL displacement in some of their interferograms. In addition, using a regularly sampled SAR data set (i.e. using every available acquisition of a regularly sampled target) will result in aliasing of the OTL signal. For example, ERS and Envisat have a repeat time of 35 days giving an aliased period of 95.3 days for the M2 (principal lunar semi-diurnal) tidal constituent.

[12] Figures 2 and 3 show predicted displacements in the radar line of sight (LOS) direction as they would be measured by InSAR due purely to the OTL for northern Iceland and Peru respectively. These displacements were produced by calculating the OTL displacement projected into the LOS and differencing the displacement for the two acquisition times. InSAR measurements have a constant shift ambiguity and only relative displacements within the image are actually measured; therefore to facilitate intercomparisons we remove the median displacement from both Figures 2 and 3. The use of wide swath radar images has become more common with the current generation of SAR satellites. Wide swath images have a lower resolution but provide a swath width about three times larger than the normal strip-map swath width, and are thus useful for capturing an entire plate boundary in a single image [e.g., *Simons and Rosen*, 2007]. For satellite tracks parallel to the coastline a wide swath image is expected to have a larger relative OTL displacement compared to a normal swath image. In Figure 3 the across track OTL displacement for the wide swath image is over 26 millimeters while the deformation across the strip-map image is about 12 millimeters.

[13] We expect the OTL to map into the baseline re-estimation if it is not removed prior to the re-estimation process. Typical OTL displacements will result in baseline re-estimation errors of up to 0.5 m, which is larger than the precision of reported orbits. If the baseline is not re-estimated during processing, then it is common to estimate a bi-linear ramp from the interferogram during modelling.

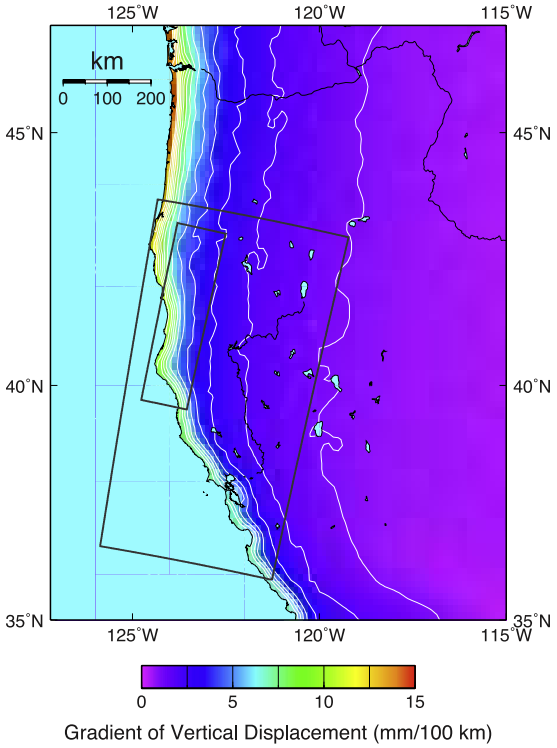

Figure 4. Magnitude of the horizontal gradient of the vertical OTL displacement of the M2 constituent for the western United States. Boxes show characteristic footprints of wide swath and strip-map images. Contour intervals are 1 mm/100 km.

Figures 2 and 3 also show residual displacements after removing a best fitting bi-linear ramp.

[14] The influence of the OTL on displacement gradients will decrease away from the coast. For any particular geographic region, the horizontal gradient in OTL displacements across the interferogram is a measure of the sensitivity of the interferogram to the OTL. Figure 4 shows the magnitude of the horizontal gradient in the vertical displacement amplitude of the OTL due to the M2 tidal constituent for the western United States which is tectonically active both near the coast and several hundreds of kilometers inland (the M2 being the largest constituent and the vertical displacement having the largest effect on an interferogram). More than about 200 km away from the coast the OTL gradient is relatively small.

3. Conclusions

[15] As InSAR is more commonly used as a high precision geodesy technique for small amplitude, long-wavelength processes, the correct treatment of the ocean tidal load becomes important. We have shown that the size of the OTL displacement is comparable to both InSAR accuracy and rate of deformation for scientifically interesting targets near coastlines. The OTL correction is relatively insignificant if the target is large, rapid deformation (e.g. co-seismic studies); however, when investigating smaller amplitude displacement processes the OTL should be considered. The orbits of the SAR satellites may be known well enough that orbit re-estimation is not necessary and we can therefore recover long-wavelength features previously ignored in InSAR analysis. Even when baseline re-estimation removes the long-wavelength ramp from an interferogram, the OTL can map into baseline errors and should therefore be removed prior to such processing.

[16] **Acknowledgments.** We thank Duncan Agnew for providing the SPOTL software and assistance in using it, Mathilde Vergnolle for advice on tidal models, and Eric Fielding for providing the wide swath radar geometry. The manuscript was improved by comments from an anonymous reviewer. We are very grateful to Nigel Penna whose detailed comments greatly improved this manuscript. This work is supported in part by the Gordon and Betty Moore Foundation and NASA grant NNG06GFR47G. This is Caltech Seismological Laboratory Contribution 10002 and Caltech Tectonic Observatory Contribution 83.

References

Agnew, D. C. (1997), NLOADF: A program for computing ocean-tide loading, *J. Geophys. Res.*, *102*, 5109–5110.

Agnew, D. C. (2007), Earth tides, in *Treatise on Geophysics*, vol. 3, edited by T. Herring, chap. 6, pp.163–195, Elsevier, New York.

Baker, T. F., and M. S. Bos (2003), Validating Earth and ocean tide models using tidal gravity measurements, *Geophys. J. Int.*, *152*, 468–485.

Blewitt, G. (2007), GPS and space-based geodetic methods, in *Treatise on Geophysics*, vol. 3, edited by T. Herring, chap. 11, pp. 351–390, Elsevier, New York.

Bos, M., and T. Baker (2005), An estimate of the errors in gravity ocean tide loading computations, *J. Geod.*, *71*, 50–63, doi:10.1007/s00190-005-0442-5.

Dong, D., P. Fang, Y. Bock, M. K. Cheng, and S. Miyazaki (2002), Anatomy of apparent seasonal variations from GPS-derived site position time series, *J. Geophys. Res.*, *107*(B4), 2075, doi:10.1029/2001JB000573.

Eanes, R., and S. Bettadpur (1995), The CSR 3.0 global ocean tide model, *Tech. Memo. CSR-TM-96-05*, Cent. for Space Res., Univ. of Tex. at Austin, Austin.

Egbert, G. D., and S. Y. Erofeeva (2002), Efficient inverse modeling of barotropic ocean tides, *J. Atmos. Oceanic Technol.*, *19*, 183–204.

Farrell, W. E. (1972), Deformation of Earth by surface loads, *Rev. Geophys. Space. Phys.*, *10*, 761–797.

Lefevre, F., F. H. Yard, C. Le Provost, and E. J. O. Schrama (2002), FES99: A global tide finite element solution assimilating tide gauge and altimetric information, *J. Atmos. Oceanic Technol.*, *19*, 1345–1356.

Matsumoto, K., T. Takanezawa, and M. Ooe (2000), Ocean tide models developed by assimilating TOPEX/POSEIDON altimeter data into hydrodynamical model: A global model and a regional model around Japan, *J. Oceanogr.*, *56*, 567–581.

Matsumoto, K., T. Sato, T. Takanezawa, and M. Ooe (2005), GOTIC2: A program for computation of oceanic tidal loading effect, *J. Geod. Soc. Jpn.*, *47*, 243–248.

Melachroinos, S. A., et al. (2007), Ocean tide loading (OTL) displacements from global and local grids: Comparisons to GPS estimates over the shelf of Brittany, France, *J. Geod.*, *82*, 357–371, doi:10.1007/s00190-007-0185-6.

Penna, N., M. King, and M. Stewart (2007), GPS height time series: Short-period origins of spurious long-period signals, *J. Geophys. Res.*, *112*, B02402, doi:10.1029/2005JB004047.

Penna, N. T., M. S. Bos, T. F. Baker, and H.-G. Scherneck (2008), Assessing the accuracy of predicted ocean tide loading displacement values, *J. Geod.*, doi:10.1007/s00190-008-0220-2.

Ray, R. (1999), A global ocean tide model from TOPEX/POSEIDON altimetry: GOT99.2, *NASA Tech. Memo., NASA/TM-1999-209478*.

Scherneck, H. G. (1991), A parametrized solid Earth tide model and ocean tide loading effects for global geodetic base-line measurements, *Geophys. J. Int.*, *106*, 677–694.

Simons, M., and P. Rosen (2007), Interferometric synthetic aperture radar geodesy, in Treatise on Geophysics, vol. 3, edited by T. Herring, chap. 12, pp. 391–446, Elsevier, New York.

Thomas, I. D., M. A. King, and P. J. Clarke (2007), A comparison of GPS, VLBI and model estimates of ocean tide loading displacements, *J. Geod.*, *81*, 359–368, doi:10.1007/s00190-006-0118-9.

Urschl, C., R. Dach, U. Hugentobler, S. Schaer, and G. Beutler (2005), Validating ocean tide loading models using GPS, *J. Geod.*, *78*, 616–625.

Vergnolle, M., M.-N. Bouin, L. Morel, F. Masson, S. Durand, J. Nicolas, and S. A. Melachroinos (2008), GPS estimates of ocean tide loading in NW-France: Determination of ocean tide loading constituents and comparison with a recent ocean tide model, *Geophys. J. Int.*, *173*, 444–458, doi:10.1111/j.1365-246X.2008.03734.x.

C. J. DiCaprio and M. Simons, Seismological Laboratory, California Institute of Technology, MS 252-21, Pasadena, CA 91125, USA. (dicaprio@gps.caltech.edu; simons@caltech.edu)